Biochimica et Biophysica Acta 1851 (2015) 261–272

Contents lists available at ScienceDirect

Biochimica et Biophysica Acta

journal homepage: www.elsevier.com/locate/bbalip

Two sites of action for PLD2 inhibitors: The enzyme catalytic center and an allosteric, phosphoinositide biding pocket

Ramya Ganesan, Madhu Mahankali, Gerald Alter, Julian Gomez-Cambronero *

Department of Biochemistry and Molecular Biology, Wright State University School of Medicine, Dayton, OH 45435, USA

ARTICLE INFO

Article history:
Received 30 August 2014
Received in revised form 2 December 2014
Accepted 9 December 2014
Available online 20 December 2014

Keywords:
Cancer
Catalysis
Protein structure
Phosphoinositide
Lipid signaling

ABSTRACT

Phospholipase D (PLD) has been implicated in many physiological functions, such as chemotaxis and phagocytosis, as well as pathological functions, such as cancer cell invasion and metastasis. New inhibitors have been described that hamper the role of PLD in those pathologies but their site of action is not known. We have characterized the biochemical and biological behavior of the PLD1/2 dual inhibitor 5-Fluoro-2-indolyl des-chlorohalopemide (FIPI), and the specific PLD2 inhibitor, N-[2-[1-(3-Fluorophenyl)-4-oxo-1,3,-8-triazaspiro[4.5]dec-8-yl]ethyl]-2-naphthalenecarboxamide (NFOT), and found that both FIPI and NFOT are mixed-kinetics inhibitors. Mutagenesis studies indicate that FIPI binds at S757 of PLD2, which is within the HKD2 catalytic site of the enzyme, whereas NFOT binds to PLD2 at two different sites, one being at S757/S648 and another to an allosteric site that is a natural site occupied by PIP_2 (R210/R212). This latter site, along with F244/L245/L246, forms a hydrophobic pocket in the PH domain. The mechanism of action of FIPI is a direct effect on the catalytic site (and as such inhibits both PLD1 and PLD2 isoforms), whereas PLD2 affects both the catalytic site (orthosteric) and blocks PIP_2 binding to PLD2 (allosteric), which negates the natural enhancing role of PIP_2. Moreover, NFOT prevents cell invasion of cancer cells, which does not occur in cells overexpressing PLD2-F244A/L245A/L246A, or PLD2-R210A/R212A, or PLD2-S757/S648 mutants. This study provides new specific knowledge of enzyme regulation and mechanisms of activation and inhibition of PLD2 that are necessary to understand its role in cell signaling and to develop new inhibitors for cancer cell invasion and metastasis.

1. Introduction

Phospholipase D (PLD) is a hydrolytic enzyme that catalyzes the conversion of phosphatidylcholine (PC) to produce free acid, phosphatidic acid (PA), and choline. Phospholipase D belongs to the HKD superfamily that has one or two "H-x-K-x(4)-D" motifs in its catalytic site. This HKD motif accounts for the lipase activity of Phospholipase D. There are 6 isoforms of mammalian PLD, namely, PLD1–6. PLD1 and PLD2 belong to the classical HKD superfamily that possesses phosphoinositide binding (PX) and pleckstrin homology (PH) domains with 2 HKD motifs, while PLD3–6 and bacterial cardiolipin synthase belong to the non-classical HKD superfamily that lack PX and PH domains and may have 1 or 2 HKD motifs. The PX and PH domains of PLD are the major regulatory domains of PLD. However, there are studies showing the C-terminus of PLD also has binding regions for small GTPases such as ARF and Rho, which functions in a regulatory role [6,32].

The PX is a phosphointositide (PI)-binding domain involved in targeting of proteins to cell membranes. The PX domain was first identified in p40phox and p47phox of NADPH oxidase and later was also found in many PI3 kinases [20,30]. The PH domain is approximately 120 amino acid sequence that occurs in many proteins that are involved in signaling or are constituents of cytoskeleton. This domain can bind PI lipids within the membrane [28], big subunits of heterotrimeric G-proteins such as receptor tyrosine and serine/threonine kinases [29] and protein kinase C [33]. The PLD2-PH domain is known to interact with phosphoinositide 4,5-bisphosphate (PtdIns (4,5)P_2) (PIP_2), and this interaction is important for the intracellular localization of PLD2 [8,9,23].

The product of its enzymatic reaction carries many of the functions of PLD in cell signaling and it is involved in cellular signaling and membrane dynamics in all eukaryotes [12]. Thus, PA binds to ribosomal S6 kinase (S6K) and leads to subsequent actin polymerization and chemotaxis, for leukocytes [14]. PA interacts with many other proteins such as mTOR, Sos [36], Rac and Ras [19]. PA also interacts with Sos through Grb2 activating the Erk/MAPK pathway [36] culminating in DNA synthesis [2]. PA serves as a precursor for bioactive lipids such as LPA and DAG.

* Corresponding author at: Department of Biochemistry and Molecular Biology, Wright State University School Medicine, 3640 Colonel Glenn Highway, Dayton, OH 45435, USA. Fax: +1 937 775 3730.
E-mail address: julian.cambronero@wright.edu (J. Gomez-Cambronero).

http://dx.doi.org/10.1016/j.bbalip.2014.12.007

Table 1
Table showing list of existing PLD inhibitors, their abbreviations, chemical structure and isoform specificity. Also mentioned are the IC_{50} values.

PHOSPHOLIPASE D (PLD) INHIBITORS			
IUPAC name	Abbrev. name	Chemical structure	Isoform specificity
N-[2-[1-(3-Fluorophenyl)-4-oxo-1,3,-8-triazaspiro[4.5]dec-8-yl]ethyl]-2-naphthalenecarboxamide. [13]	NFOT	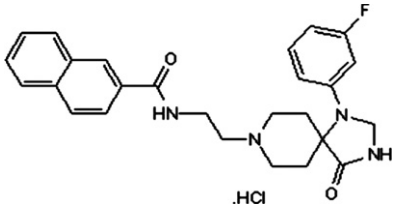	PLD2 inhibitor
N-[2-(4-oxo-1-phenyl-1,3,8-triazaspiro[4,5]dec-8-yl)ethyl]-2-naphthalenecarboxamide. [37]	NOPT	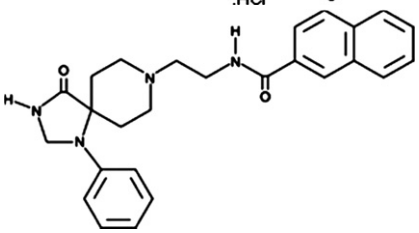	PLD2 inhibitor
N-[2-[4-(5-chloro-2,3-dihydro-2-oxo-1H-benzimidazol-1-yl)-1-piperidinyl]-1-methylethyl]-2-naphthalenecarboxamide. [37]	NBOD	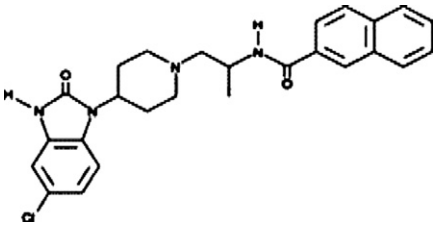	PLD1 inhibitor
(1R,2R)-N-([S]-1-{4-[5-bromo-2-oxo-2,3-dihydro-1H-benzo(d)imidazol-1-yl]piperidin-1-yl} propan-2-yl)-2- phenylcyclopropanecarboxamide. [37]	RBPC	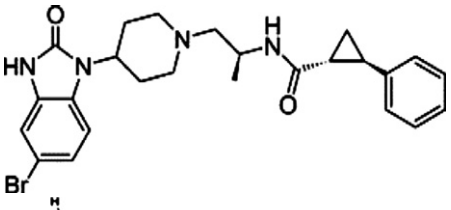	PLD1 inhibitor
N-[2-[4-(2,3-Dihydro-2-oxo-1H-benzimidazol-1-yl)-1-piperidinyl]ethy]-5-fluoro-1H-indole-2-carboxamide; other name: 5-Fluoro-2-Indolyl des-Chlorohalopemide. [26]	FIPI	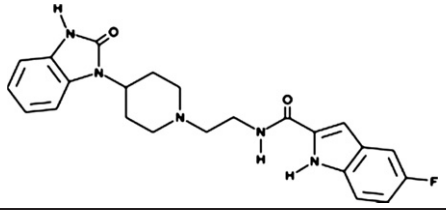	Dual (PLD1 and PLD2) inhibitor

A role of PLD in cancer has been stated repeatedly. High levels of PLD2 expression were observed in patients with colorectal cancer [18,21]. A polymorphism in PLD2 1814 C ➔ T causing a mutation, Ile577Thr, was predominant in colorectal cancer patients, but this polymorphism did not affect PLD activity [31]. Previous studies have shown that inhibiting PLD1 in the tumor microenvironment by FIPI dampens metastasis and angiogenesis [1]. On the other hand, involvement of PLD2 in tumor metastasis and invasion was also reported, wherein, it was shown that NOPT (a specific PLD2 inhibitor) inhibited tumor metastasis and cell invasion in xenograft mice models [7].

Based on the large array of functionalities ascribed to PLD, it is no surprise that inhibitors are necessary to probe this field further. New and powerful PLD inhibitors have been synthesized that in many cases are derivatives of halopemide (Table 1) [1,13,17,24,25]. These inhibitors show greater inhibition *in vitro*, while their bioavailability *in vivo* is reduced due to the properties of the drug, including hydrophobicity and solubility. Monovich et al. showed that the half-life of FIPI in vivo is 5.5 hours and the bioavailability is only 18% [17].

To date, there is no clear site of action of these specific small-molecule inhibitors on PLD2 and/or their mechanism of action. This study reports that the PLD2 inhibitor NFOT uses an allosteric site, which overlaps with PIP_2 binding sites of the PH domain, to target its activity. The importance of this is that knowledge about the mechanism and kinetics of the existing inhibitors will help in developing more potent PLD inhibitors to be used in pathological conditions.

2. Materials and methods

2.1. Materials

The COS-7, African black monkey kidney fibroblasts were purchased from ATCC. COS-7 culture medium Dulbecco's modified eagle medium (DMEM), Fetal Bovine Serum and TransfectaGRO were obtained from Corning Cellgro® (Manassas, VA). Lipofectamine, Plus, and EGF were purchased from Invitrogen (Carslbad, CA). 3[H]- butanol was obtained from Perkin Elmer (Waltham, MA). All the phospholipids required for lipase enzyme activity assays including PC8 and PIP_2 were purchased from Avanti Polar Lipids. Matrigel inserts were purchased from BD (Franklin Lakes, NJ). Hematoxylin stain was obtained from Ricca (Arlington, TX). Phospholipase D (PLD) inhibitors were obtained from Cayman Chemicals, Avanti polar lipids and Tocris biosciences.

2.2. Cell culturing and Plasmid transfections

COS-7 cells were cultured and sub-cultured in DMEM with 10% FBS, 50 U/ml Penicillin, 50 U/ml Streptamycin, and 50 μg/ml Gentamycin at 37 °C temperature and 5% carbon-dioxide in a CO_2 incubator. Cells were split at 80% confluence. The cells were transfected at 60% confluence per well with plasmids ranging from 1–6 μg of DNA, using 6 μl Lipofectamine and 6 μl Plus diluted in 600 μl TransfectaGRO. Sterile glass culture tubes housed each aliquoted liposome solution (DNA + Lipid complex) prior to transferring the solution into 6-well plates of cells containing 1 ml of TransfectaGRO. The transfection mix was allowed for 3 hours and then the media was aspirated and changed to fresh complete DMEM. Transfection was allowed to go for 48 hours.

2.3. Phospholipase activity assay

PLD2 was processed for lipase activity as mentioned in refs. [3,7,10,14,15,34]. Briefly, the assay was performed in liposomes of 1,2-dioctanoyl-*sn*-glycero-3-phosphocholine (PC8) and [^{3}H]-butanol. The following reagents (final concentrations): 3.5 mm PC8 phospholipid, 45 mm HEPES, pH 7.8, and 1.0 μCi of n-[^{3}H]-butanol were added in a liposome form as indicated in ref. [15]. Samples were incubated for 20 min at 30 °C with continuous shaking. The addition of 0.3 ml of ice-cold chloroform/methanol (1:2) stopped the reactions. Lipids were isolated, dried (under N_2), and resuspended in chloroform:methanol (9:1) and then spotted on thin-layer chromatography plates along with phospholipid controls 1,2-dioleoyl-sn-glycero-3-phosphoethanolamine (p-ethanol) and 1,2-dipalmitoyl-sn-glycero-3-phosphobutanol (p-butanol) (Avanti polar lipids, Inc., AL). The amount of [^{3}H]-phosphatidylbutanol ([^{3}H]-PBut) that co-migrated with PBut standards was measured by scintillation spectrometry. Whole cells were assayed quite similar to the lysates, except that the cells were first treated with inhibitor for 25 min at 37 °C. Followed by inhibitor treatment, lysates were prepared and subjected to lipase activity assay.

2.4. Generation of purified PLD2

A baculovirus expression system was used for the overexpression and subsequent purification of recombinant, full-length PLD2 for use in certain enzymatic reactions. Briefly, the PLD2-WT gene and the Bsu36I-digested BacPAK5 viral DNA were co-transfected into Sf21 insect cells in separate reactions, which rescued the very large viral DNA and effectively transferred the PLD2 gene into the AcMNPV genome. PLD2 baculoviral stock that overexpressed PLD2-WT was selected and used to infect Sf21 insect cells for further overexpression of PLD2 and enrichment of PLD2 using a TALON matrix, as described in ref. [4].

2.5. Enzyme inhibition assay

Cells were cultured and transfected with PLD1 or PLD2, 48 h post-transfection, cells were starved for 2 h, stimulated with EGF (3 nM), and cells lysates were prepared. For some experiments (named "whole cells"), whole cells were treated with inhibitors prior making lysates, or cell lysates were treated directly with the inhibitors (named "lysates"). At any case, the treatment was 300 nM (unless otherwise indicated) PLD1 inhibitor (NBOD), PLD2 (NFOT) inhibitor and dual inhibitor (FIPI) for 25 min. After treatment with the inhibitor, the lysates were prepared and taken to lipase activity assay as mentioned above, but with increasing concentrations of PC8, which is the substrate of PLD. The phospholipase activity of the enzyme was measured by measuring the radioactivity in a scintillation counter.

2.6. Western blotting

Lysates were prepares in the desired volume of Special lysis buffer (50 mM HEPES, pH 7.2, 100 μM Na_3VO_4, 0.1% Triton X-100, and 1 mg/ml each of protease inhibitors (aprotonin and leupeptin) and then sonicated. The BIO-RAD protein estimation assay was utilized to determine the protein concentration and to normalize among preparations to ensure equal protein content per reaction. The desired concentration of protein was loaded into the wells of SDS–PAGE gels along with a molecular weight marker. These gels were then transferred for 1 h onto PVDF membrane, blocked for 45 min at room temperature with 1% BSA with TBS, 0.2% Tween 20 (TBS-T), and probed with primary antibody overnight. The blots were then washed with TBS-T and probed with secondary antibody conjugated to horseradish peroxidase (HRP) and detected on x-ray films with the help of ECL western blotting detection reagents from GE Health Care (Fairfield, CT). The Kodak Gel Logic software used to perform densitometry on western blots, which consists of quantifying the band of the protein of interest versus the band of the actin-loading control.

2.7. Cell migration and cell invasion

Adherent cells were detached using 25% Trypsin/EDTA or a non-enzymatic cell dissociation buffer for COS-7 or RAW264.7 cells, respectively. A hemocytometer was used to count cells, and trypan blue exclusion was used to determine cell viability. 24-well plates and Transwell inserts were pre-wetted with DMEM containing 0.5% BSA. Cell concentration was adjusted to 5×10^4 cells per 400 μl of DMEM containing 0.5% BSA per insert. 600 μl of DMEM containing 5% BSA was added to the bottom of the well prior to placing the cells and insert in the well. Three nanomolar EGF for COS-7 cells or 3 nM M-CSF for RAW264.7 cells were used as chemoattractants, respectively. The murine macrophage cells were allowed to migrate for 3.5 h and COS-7 cells migrated for 1 h at 37 °C, 5% CO_2. Afterward, inserts were removed and cells that had migrated to the bottom were fixed with 4% paraformaldehyde in each well. Cells that migrated to the bottom were then allowed to settle and adhere before being counted. Cells were then counted using an inverted microscope at 20×. The average numbers of 6 counts per well were counted and statistics performed. Cell invasion was conducted using Matrigel inserts.

2.8. Prediction of full-length PLD2 structure: homology modeling

Full-length PLD2 structure model was obtained as explained in ref. [16]. Briefly, the primary sequence of PLD2 was submitted to the protein prediction servers, I-TASSER (Iterative threading assembly refinement) [35] and Phyre 2 (protein homology/analogy recognition engine) [11] servers. The molecular modeling and visualization of the structure model was performed using the Swiss PDB viewer (SPDBV) [5]. Multiple candidate structures were analyzed to select the final structure. By visual inspection, we concluded the PLD2 model predicted by Phyre2 server meets most of the set criteria that were based on the experimental findings from the literature. However, the model was still not entirely energetically favorable as certain amino acid conformations were not reasonable. These issues were fixed by manually perturbing the structure using SPDBV and energy minimizing the resulting structure(s) using steepest descent and conjugate gradient methods. Finally, the complete 3D model was energy minimized which resulted in a model, which was energetically favorable and consistent with experimental criteria.

2.9. Molecular docking

The computer-simulated docking studies were performed using AutoDock Vina [27], which allows rotation about ligand in order to have flexible/rotatable bonds. Docking with *AutoDock Vina* starts by defining a search space or binding site in a restricted region of the protein. In order to dock the small-molecule inhibitors with our PLD2 structure model, a receptor grid was generated including the two catalytic histidines (442 and 756) in our 3D model. The resulting ligand conformation was further visualized using the PyMOL. Regarding to the structures of

the inhibitors, structural information was take from PubChem or Cayman chemicals and 3D models built in used SPDBV Swiss Protein Data Bank Viewer.

2.10. Statistical Analysis

Data are presented as the mean ± SEM. The difference between means was assessed by the single-factor analysis of variance (ANOVA) test. Probability of $p < 0.05$ was considered to indicate a significant difference.

3. Results

3.1. Characterizing the existing PLD inhibitors

The goal of this study is to obtain information from the existing PLD inhibitors regarding the type of the inhibitors and the site of their action. This will further allow the development of specific and efficient inhibitors. PLD inhibitors available are either PLD1 specific or PLD2 specific or dual inhibitors. However, the type of these inhibitors as in whether they are competitive or non-competitive or mixed, is not clear. Therefore we sought to characterize the type of existing efficient inhibitors.

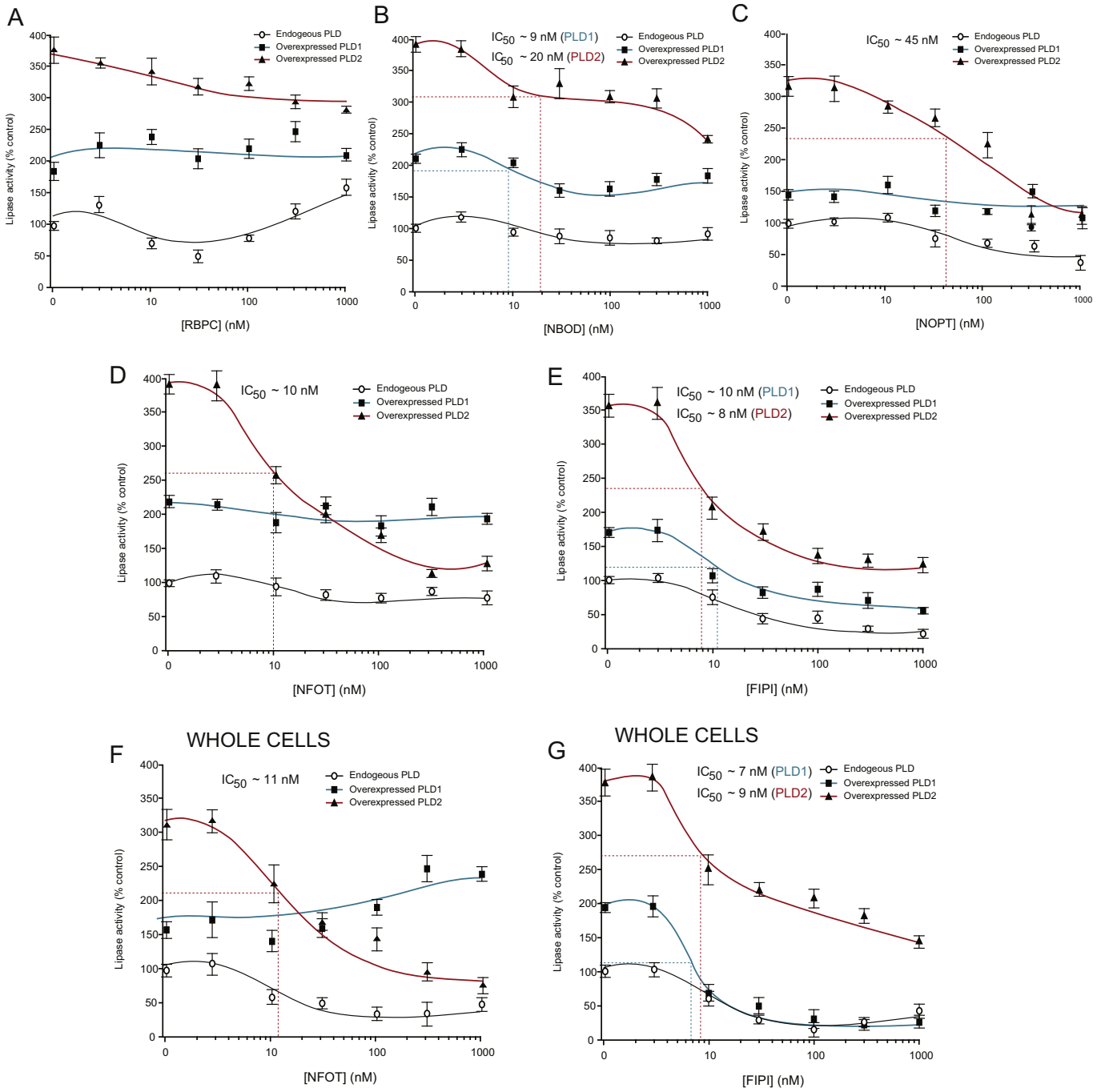

Fig. 1. Determination of IC50 values of the inhibitors listed in Table 1. COS7 cells were untransfected or transfected with PLD1 or PLD2. Post transfection, cell lysates were treated with increasing concentrations of inhibitor ranging from 0 to 1 μM and lipase assay was performed. Shown is the dose–response curve of PLD1 specific inhibitors (A) RBPC and (B) NBOD, PLD2 specific inhibitors (C) NOPT and (D) NFOT. (E) Dual inhibitor FIPI has an IC_{50} of 30 and 20 nM for PLD1 and PLD2 respectively. Intact cells were treated with increasing concentrations of (F) NFOT and (G) FIPI. For each inhibitor, and for each transfection we considered the maximum level of the enzyme activity at zero inhibitor and then the minimum activity at the maximum concentration of inhibitor used (1 micromolar), identified the 50% activity and extrapolated the concentration for this IC_{50}.

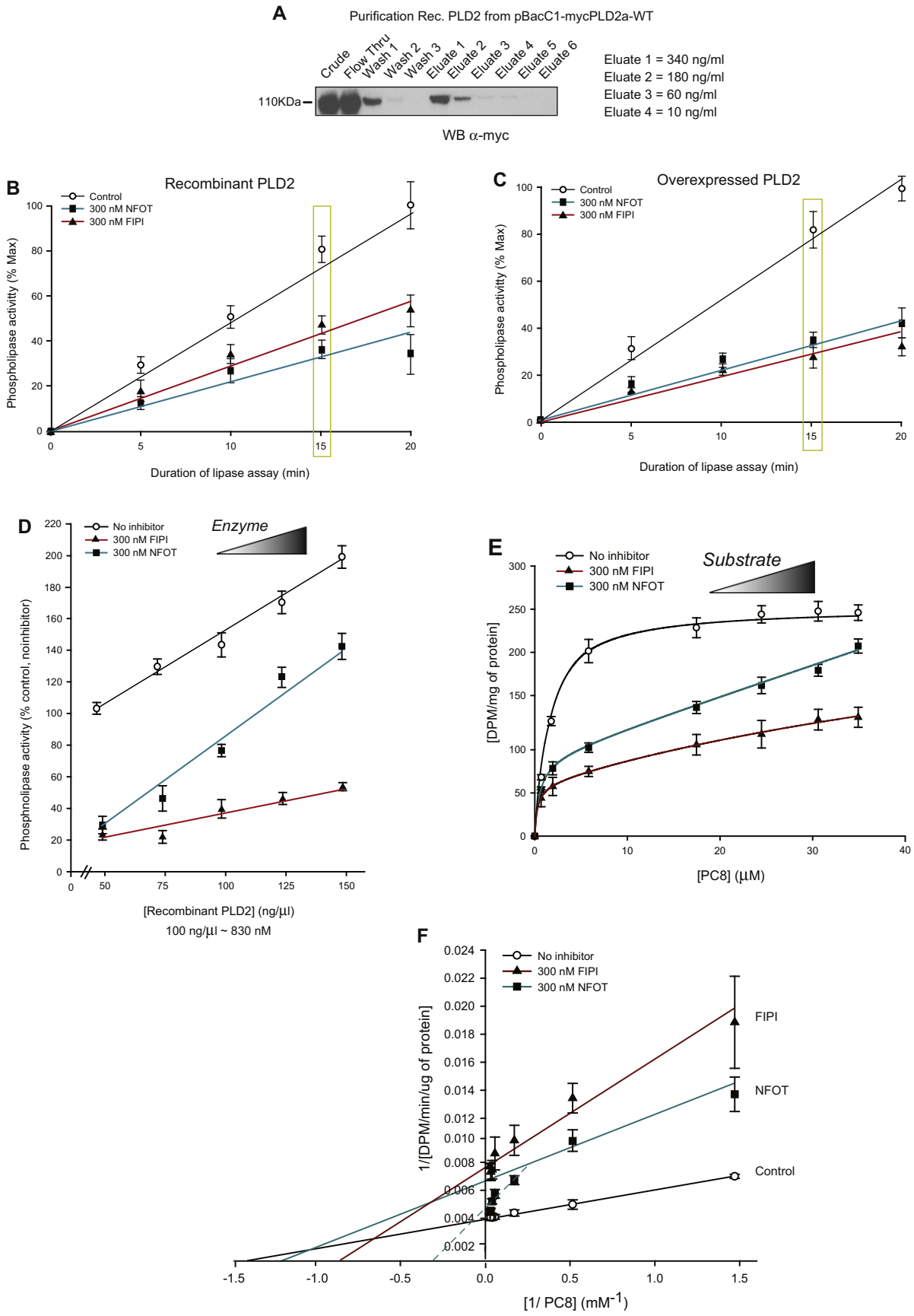

Fig. 2. Characterization of PLD inhibitors FIPI and NFOT. (A) Western blot analysis of PLD2 purification. (B) Determination of linearity for PLD2 activity and inhibition. (C) Increasing concentrations of purified recombinant PLD2 was assayed in the absence or presence of FIPI or NFOT. (D) Shown is the Michaelis–Menten kinetics plot of FIPI and NFOT respective to the control. E) Shown is the Lineweaver–Burke plot of FIPI and NFOT respective to the control. A second line could be derived in NFOT experimental points if one considers high concentration of substrate (>10 mM). This is indicated by a dashed line in panel E.

The inhibitors we used in this study are NFOT (PLD2 specific), NOPT (PLD2 specific), NBOD (PLD1 specific), RBPC (PLD1 specific), and FIPI (dual). The details and systematic names are listed in Table 1. In order to verify the potency and specificity of the inhibitors to the targets, the IC50 of the listed inhibitors were determined (Fig. 1D–G). In our hands, NBOD and specially RBPC did not efficiently inhibit PLD activity in PLD1 overexpressed samples. On the contrary, PLD2 was potently inhibited by both NFOT (EC50 ~ 10 nM in both whole cells an lysates)

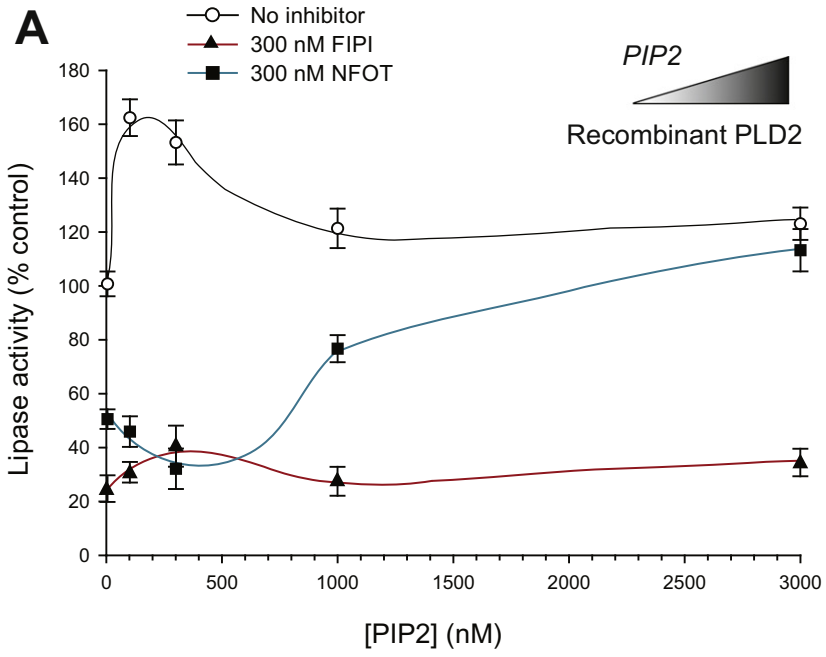

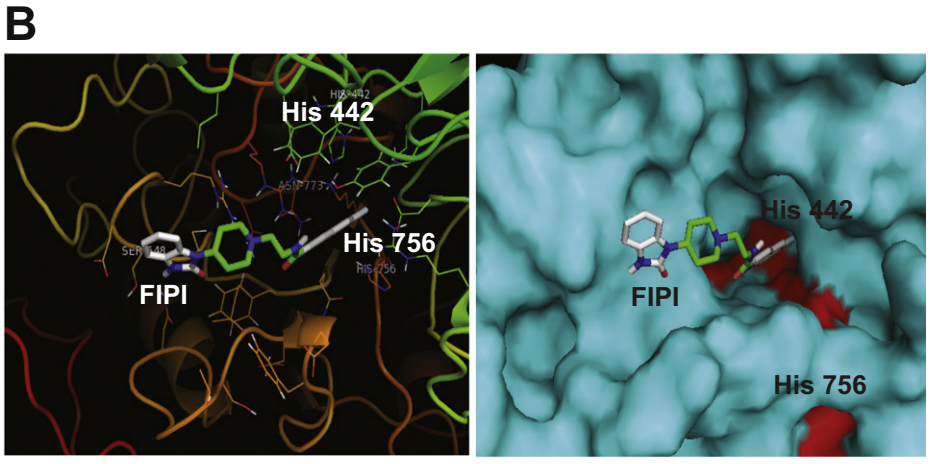

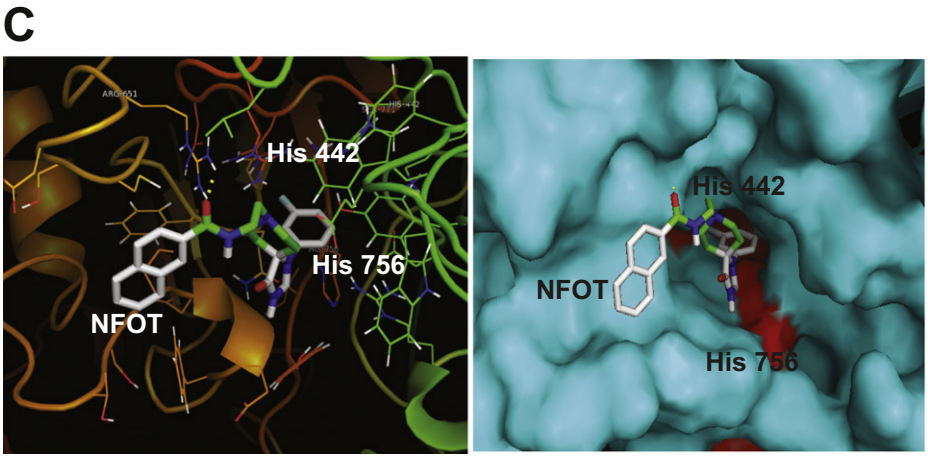

Fig. 3. Kinetics of PLD2 inhibition in the presence of allosteric regulator, PIP_2. PLD2 was subjected to lipase activity assay with increasing concentrations of PIP_2 in the presence or absence of FIPI or NFOT. Panels B (ribbon) and C (surface) show the modeling of both inhibitors biding to the PLD enzyme. Colored in red are the Histidine residues.

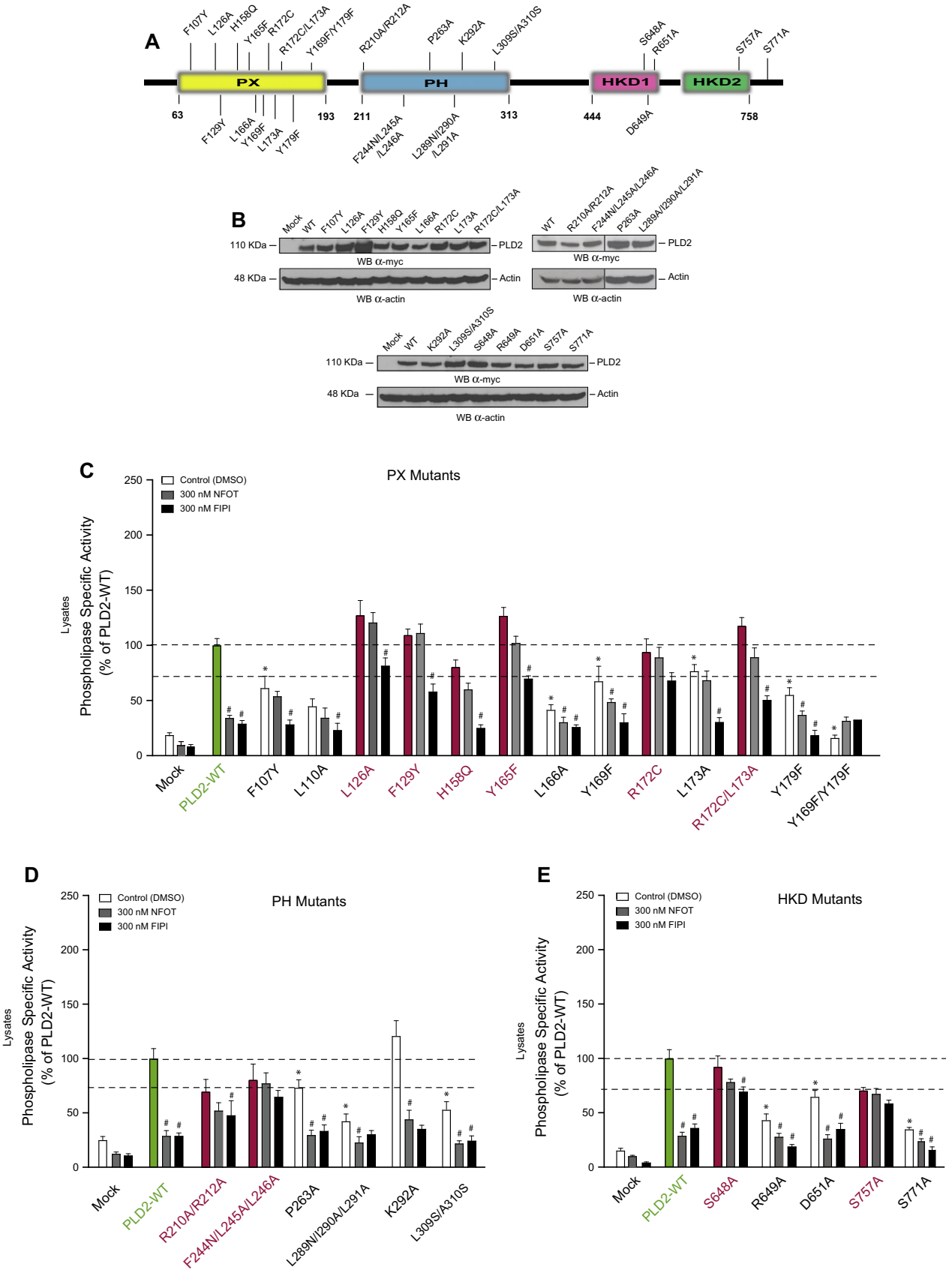

Fig. 4. Mutagenesis analysis. (A) Schematic representation of the various mutations in PLD2. (B) Western blot analysis of mutants overexpressed in COS7 cells. Lipase activity assay was performed with all the mutants in the (C) PX, (D) PH, and (E) HKD regions in the absence or presence of NFOT or FIPI. Mutants that had 75 % or more activity (2nd dashed line) compared to WT were shown in red bars. L126A, F129Y, Y165F, R172C, and R172C/L173A in the PX and S648 near HKD regions were partially resistant to inhibition by NFOT. Statistically significant ($p < 0.05$) SEM compared to PLD2-WT controls are denoted by an asterisk (*). Statistically significant ($p < 0.05$) SEM compared to each PLD2 mutant in each group denoted by a hash-tag (#).

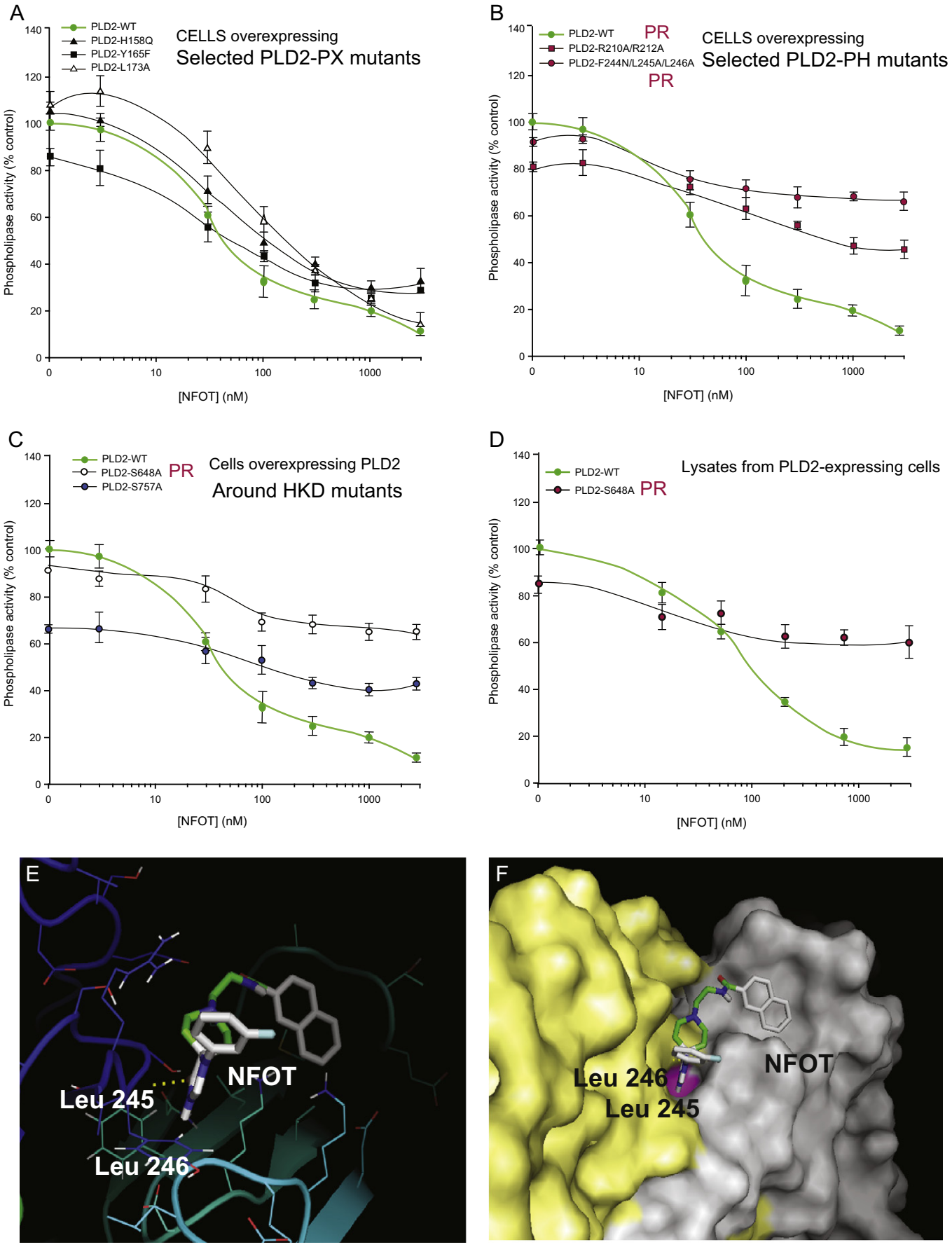
A
PLD2-WT
PLD2-H158Q
PLD2-Y165F
PLD2-L173A
CELLS overexpressing
Selected PLD2-PX mutants
Phospholipase activity (% control)
[NFOT] (nM)
B
PLD2-WT
PR
PLD2-R210A/R212A
PLD2-F244N/L245A/L246A
PR
CELLS overexpressing
Selected PLD2-PH mutants
Phospholipase activity (% control)
[NFOT] (nM)
C
PLD2-WT
PLD2-S648A
PR
PLD2-S757A
Cells overexpressing PLD2
Around HKD mutants
Phospholipase activity (% control)
[NFOT] (nM)
D
PLD2-WT
PLD2-S648A
PR
Lysates from PLD2-expressing cells
Phospholipase activity (% control)
[NFOT] (nM)
E
NFOT
Leu 245
Leu 246
F
Leu 246
Leu 245
NFOT

and FIPI (EC50 ~ 8–9 nM). FIPI affected also PLD1 (EC50 ~ 7–10 nM). In all cases, endogenous PLD activity was also inhibited. The results in Fig. 1 indicate that NFOT and FIPI are efficient, and hence these two inhibitors were pursued for all the subsequent experiments of this study that focus on the PLD2 isoform.

3.2. FIPI and NFOT are mixed-kinetics inhibitors (affect both V_{max} and K_m)

FIPI's kinetics have been studied in ref. [26]), and we intended to ascertain the biochemical and biological behavior of FIPI and NOPT in our experiment systems. First, in order to determine the optimal time for maximal lipase activity and maximum effect of the inhibitor, a time course of the lipase assay was performed in the absence or presence of NFOT or FIPI. These experiments were performed with both recombinant protein and the cell lysates overexpressing PLD2. Recombinant PLD2 protein was purified as mentioned in ref. [4]. Fig. 2A shows the presence of PLD2 in all the fractions during purification process. Results presented in Fig. 2B and C indicate linearity and all the subsequent experiments measuring lipase activity were performed for 15 min.

We used two different approaches in order to determine if the type of inhibition exerted by FIPI or NFOT. In the first approach, increasing concentrations of the purified recombinant PLD2 was not treated or treated with 300 nM FIPI or NFOT and a fixed concentration of the substrate PC (3.5 mM) was used to perform lipase assay (Fig. 2D). In the second approach, a fixed concentration of recombinant purified PLD2 was not treated or treated with 300 nM FIPI or NFOT and the lipase assays were performed with increasing concentrations of PC (Fig. 2D, Michaelis–Menten plot). Results presented in Fig. 2, where PLD activity was regained (albeit not totally) with increasing concentrations of enzyme (Fig. 2C) or substrate (Fig. 2D), indicate that NFOT is a competitive inhibitor whereas FIPI was not totally competed off by the enzyme substrate at the concentrations used in these experiments. A Lineweaver–Burke plot (Fig. 2F) indicates that both FIPI and NFOT increase the K_m while decreasing the V_{max}, indicating a mixed-type inhibition. Further, a second line could be plotted in the case of NFOT experimental points if one considers high concentration of substrate (>10 mM). This is indicated by dashed lines in Fig. 2F and could be the first evidence that NFOT could have two sites of inhibition on PLD2.

3.3. PLD2 inhibition in the presence of PIP_2

Next, we wanted to determine the effect of PIP_2, a known positive effector of PLD2 on the action of inhibitors. Regarding the PIP_2 binding to proteins, PIP_2 binding motifs in various proteins are not well defined but generally are comprised of clusters of basic and aromatic amino acid residues. Sciorra et al. [22,23] demonstrated that R237 and W238 in the PH domain and R553 and R557 in the C-terminus of PLD2 are the binding sites for PIP_2 on PLD2. In addition, we recently identified another binding site in the PH domain of PLD2, which consists of R210 and R212 [16]. All these studies together suggest that there is a possibility that multiple PIP_2 molecules can bind the protein at the same time.

Recombinant PLD2 was untreated or treated with 300 nM FIPI or NFOT, after which the samples were subjected to lipase assay with increasing concentrations of PIP_2 and a fixed concentration of the substrate PC8. Results from vehicle treated sample (black line) suggest that PIP_2 exerts both a positive effect and a negative effect on PLD2 (Fig. 3A). A positive effect was observed at low (~100 nM) concentration of PIP_2, whereas at higher concentrations the activity returned to basal level. Even with increasing concentrations of PIP_2, FIPI inhibited the enzyme. However in the presence of NFOT the enzyme activity was regained back with increasing concentrations of PIP_2 suggesting that PIP_2 and the inhibitor might have overlapping interaction sites. Overall, this suggests that PLD2 inhibition by small-molecule compound NFOT is due to its binding to the natural site used by PLD-activator PIP_2 in addition to the catalytic site. Thus, NFOT causes both a competitive and allosteric inhibition. Modeling of putative sites of FIPI or NFOT with PLD2 3D model structure were performed using Autodock *vina*. The panels show the 3-D modeling of NFOT and FIPI as binding in the vicinity of the PLD catalytic center. In modeling, rotation was allowed between bonds in small molecules NFOT and FIPI.

3.4. The inhibitor's site on PLD2

Most or all of the existing PLD inhibitors are hydrophobic in nature that makes them highly insoluble in polar solvents, because of which it is very difficult to be able to use them in animal models. Also, the mechanism or site of action of these inhibitors is not clearly understood. Therefore we propose that elucidating the mechanism of action of these small-molecule inhibitors of PLD is essential in order to design more efficient, specific and potent inhibitors.

Our approach was to create mutants and screen them to determine the effect of the inhibitors on these mutants. We made the mutations in such a way that hydrophobic residues were mutated into less hydrophobic residues and charged amino acids such as arginine were mutated to neutral amino acids. The rationale behind this is to determine if the inhibitors require hydrophobic and charged amino acids to interact with PLD2. A battery of PLD mutants (Fig. 4A) in the PX, PH, and around HKD regions was designed in order to screen the resistance against inhibitors. Hydrophobic residues such as leucine, arginine, and tyrosine were mutated to less hydrophobic alanine. Protein expression of the PLD2 mutants is shown in Fig. 4B. All the mutants were compared with PLD2-WT in terms of the lipase activity. Mutants with 75% or more lipase activity (shown in red bars) relative to WT, and those were considered for subsequent experiments (Fig. 4C-E, 2nd dashed line).

Fig. 4 demonstrates that FIPI inhibited most of the mutants, except that PLD2-S757A was resistant to 300 nM FIPI. On the other hand, PLD2-H158Q, Y165F, and L173A in the PX domain, PLD2-R210/212A and PLD2-F244N/L245/L246A in the PH domain and PLD2-S648A and S757A in and around the HKD region demonstrated resistance against 300 nM NFOT (Fig. 4C–E). To confirm the same, these resistant mutants were subjected to increasing concentrations of NFOT (Fig. 5) or FIPI (data not shown). The results suggest that PLD2-R210A/R212A, PLD2-F244N/L245/L246A, PLD2-S648A, and PLD2-S757A are partially resistant to inhibition over a range of inhibitor concentrations of NFOT (Fig. 5A-D). Fig. 5E,F show the 3-D modeling of NFOT binding to the allosteric site in the PLD 244–246 region.

3.5. Functional relevance of the inhibitor resistant mutants

In order to determine the functional relevance of the inhibitor resistant mutants in Fig. 4 (red bars), we performed cell migration of fibroblasts (COS-7 cells) and cell invasion assays of breast cancer cells (MDA-MB-231) in the absence or presence of 300 nM, 700 nM FIPI or NFOT. The results presented in Fig. 6A and B indicate that these mutations are not affecting PLD2-mediated cell migration as well as invasion. In addition, the mutants that were observed to be resistant in Fig. 4 such as PLD2-R210A/R212A, PLD2-F244N/L245/L246A, PLD2-S648A, and PLD2-S757A are also resistant to inhibition in terms of cell migration and cell invasion and PLD2-Y165F was found to be partially resistant to inhibition in terms of chemotaxis, explaining the functional relevance.

Fig. 5. Dose-dependent effect of NFOT on the selected mutants. Mutants (A) H158Q, Y165F and L173A in the PX, (B) R210/212A and F244N/L245/L246A in the PH and (C and D) S648 near HKD were treated with increasing concentrations of NFOT and subjected to lipase assay. F244N/L245/L246A and S648A were found to be partially resistant even with increasing concentrations of NFOT. Panels E and F show the ribbon (E) and surface (F) of NFOT biding to the allosteric site in the PLD enzyme. Colored in purple are the hydrophobic residues.

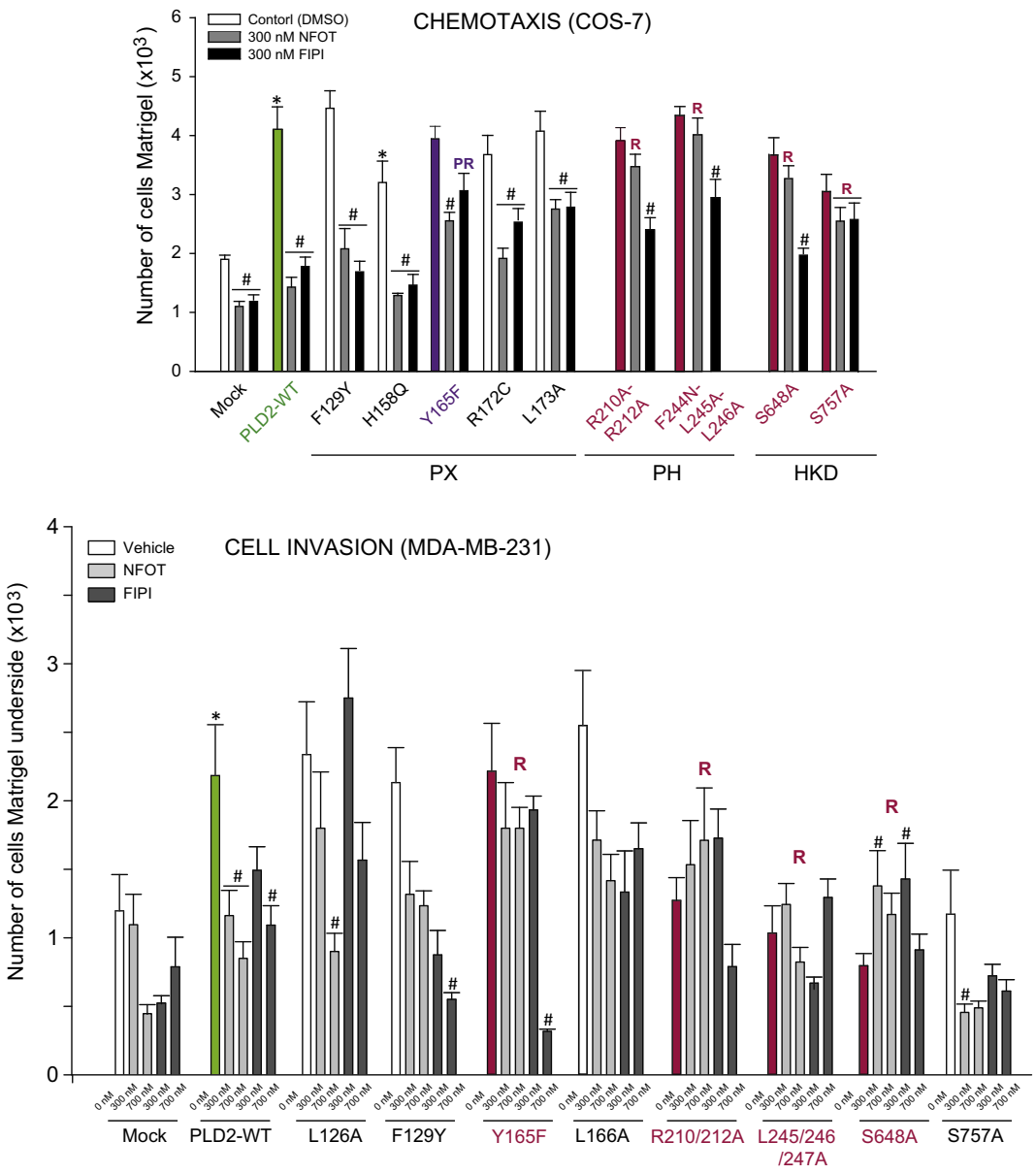

Fig. 6. Effect of inhibitors FIPI and NFOT selected PLD mutations: Functional relevance. Mutants indicated in the Figure were overexpressed in COS7 cells. Post transfection, cells were harvested, treated with inhibitors for 20 min and subjected to (A) chemotaxis or (B) cell invasion assays. Mutants, R210/212A, F244N/L245/L246A, and S648A were found to be resistant. The statistical significance marked asterisk (*) is relative to the mock lipase activity ($p < 0.05$), and the hash-tag (#) refers to any statistically significant differences ($p < 0.05$) in the lipase activity observed relative to the respective control for each experimental group.

4. Discussion

Our findings suggest that S757 is a target for FIPI inhibition and that S757/S648 as well as F244, L245, and L246 are the target of NFOT action and that mutating these key amino acid(s) results in partial resistance of the enzyme towards the inhibitor. Also, this is the first study where we have elucidated the kinetics of known PLD2 inhibitors. Lineweaver–Burke (LB) plot (Fig. 2F) shows that FIPI and NFOT inhibit PLD by increasing the K_m and decreasing V_{max} values, which therefore, might result in a mixed inhibition. Mixed inhibition suggests a wide repertoire of binding sites on PLD2, including both catalytic and regulatory regions. However, mixed inhibition of PLD2 by FIPI and NFOT does not suggest anything specific about their binding site on PLD2. To explore the site of action, we designed a battery of mutants within the PX, PH, and HKD regions of PLD2.

The data presented here suggests that FIPI is hard to be competed off by the substrate, perhaps because it may have a component of irreversible inhibitor while NFOT can be competed off easily (but not completely) by NFOT. The mutants, PLD2-F244N/L245/L246A, PLD2-R210A/R212A, and S648A are partially resistant to inhibition by NFOT (Fig. 5). Thus, the binding site of the inhibitor FIPI might be in the HKD region, which is suggestive of covalent modifications FIPI can make to PLD2. On the other hand, both HKD regions as well as PIP_2 binding regions might be the sites for NFOT's action. The fact that PLD2-F244N/L245/L246A is NFOT resistant suggests that NFOT might bind to the regulatory regions of PLD2, possibly affecting the binding of positive regulators like PIP_2 (Fig. 3). The amino acids F244, L245, and L246 are in near vicinity to the PIP_2 binding region R210 and R212 [16], suggesting that NFOT interaction overlap with PIP_2 binding to PLD2. Moreover, our data demonstrates that higher concentrations of PIP_2 can rescue PLD2 from NFOT's inhibition suggesting that NFOT does bind to the site occupied by PIP_2. NFOT is a specific PLD2 inhibitor and hence does not affect PLD1 (Fig. 1D). Based on the fact that FIPI is a dual inhibitor and our findings that it might be irreversibly inhibiting PLD2, we speculate that FIPI imparts a similar mechanism of

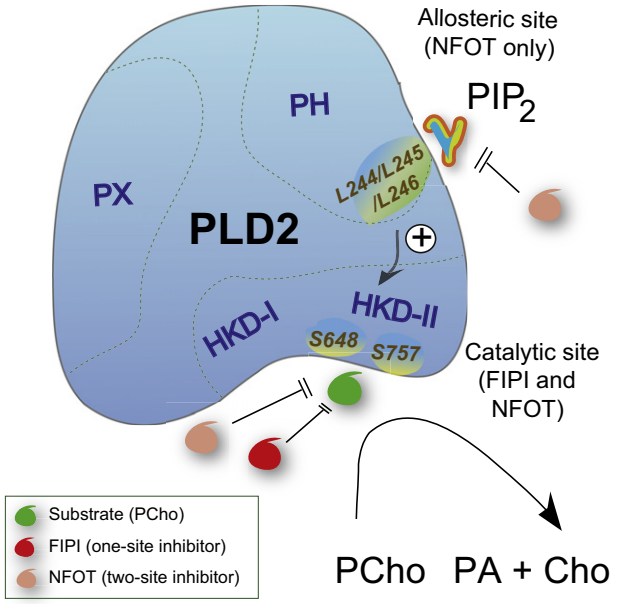

Fig. 7. A model showing the mechanism of action of FIPI and NFOT. FIPI (a dual, PLD1/PLD2-inibitro and NFOT (a PLD2-specific inhibitor) act at a site in the vicinity of the lipase catalytic site. In addition, NOFT is both a competitive and allosteric inhibitor. As indicated in this study, the possible sites of action of NFOT are F244, L245, and L246 (allosteric) in the PH region (PIP_2 binding site) and S757/S648 (orthosteric) near the HKD region, while the site of action of FIPI is S648.

inhibition on PLD1, wherein FIPI could be expected to interact with the HKD regions in the PLD molecule. FIPI might inhibit PLD1 activity irreversibly by certain covalent modifications (perhaps mediated by its fluoride moiety) not allowing complete recovery of PLD activity and its role in several physiological functions. FIPI interacts with the catalytic residues and thus imparts inhibition on both PLD1 and PLD2, which we speculate could be in part a result of a covalent modification of the enzyme molecule by the action of FIPI's fluoride moiety. We would expect a similar action of FIPI on PLD1, since it is a dual inhibitor and might interact with conserved regions on the PLD molecule.

Thus, we have developed a working model with this study showing the effect of inhibitors and the type of inhibition on PLD2 by FIPI or NFOT (Fig. 7). The model shows that NFOT binds to an allosteric site with high affinity and with comparatively low affinity to an orthosteric site (the catlytic site) on PLD2, while FIPI might cause an irreversible inhibition possibly by covalent modification of the catalytic site.

From our findings on the action of the two PLD2 inhibitors, FIPI and NFOT, one could say the two have different modes of action. FIPI could possibly act by modifying the enzyme (Figs. 1, 2E), whereas NFOT interacts at both the catalytic and allosteric sites suggesting two sites of action. The two sites for action of NFOT could possibly be accounted for by its structure wherein the fluoride possibly interacts at the catalytic site and the two benzyl rings interact at the allosteric site. Another finding from our study that would correlate with FIPI action is that the inhibition of PLD2 significantly higher than PLD1 by NBOD that also has a fluoride moiety. At any case, this study provides new specific knowledge of enzyme regulation and mechanisms of activation and inhibition of PLD2 that are necessary to understand its role in cell signaling and to develop more powerful inhibitors for cancer cell invasion and metastasis.

References

[1] Q. Chen, T. Hongu, et al., Key roles for the lipid signaling enzyme phospholipase d1 in the tumor microenvironment during tumor angiogenesis and metastasis, Sci. Signal. 5 (249) (2012) ra79.

[2] M. Di Fulvio, N. Lehman, et al., The elucidation of novel SH2 binding sites on PLD2, Oncogene 25 (21) (2006) 3032–3040.

[3] K. Frondorf, K.M. Henkels, et al., Phosphatidic acid (PA) is a leukocyte chemoattractant that acts through S6 kinase signaling, J. Biol. Chem. 285 (2010) 15837–15847.

[4] J. Gomez-Cambronero, K.M. Henkels, Cloning of PLD2 from baculovirus for studies in inflammatory responses, Methods Mol. Biol. 861 (2012) 201–225.

[5] N. Guex, M.C. Peitsch, SWISS-MODEL and the Swiss-PdbViewer: an environment for comparative protein modeling, Electrophoresis 18 (15) (1997) 2714–2723.

[6] L.G. Henage, J.H. Exton, et al., Kinetic analysis of a mammalian phospholipase D: allosteric modulation by monomeric GTPases, protein kinase C, and polyphosphoinositides, J. Biol. Chem. 281 (6) (2006) 3408–3417.

[7] K.M. Henkels, G.P. Boivin, et al., Phospholipase D (PLD) drives cell invasion, tumor growth and metastasis in a human breast cancer xenograph model, Oncogene 32 (2013) 5551–5562.

[8] M.N. Hodgkin, M.R. Masson, et al., Phospholipase D regulation and localisation is dependent upon a phosphatidylinositol 4,5-biphosphate-specific PH domain, Curr. Biol. 10 (1) (2000) 43–46.

[9] A. Honda, M. Nogami, et al., Phosphatidylinositol 4-phosphate 5-kinase alpha is a downstream effector of the small G protein ARF6 in membrane ruffle formation, Cell 99 (5) (1999) 521–532.

[10] J.M. Horn, J.A. Lehman, et al., Presence of a phospholipase D (PLD) distinct from PLD1 or PLD2 in human neutrophils: immunobiochemical characterization and initial purification, Biochim. Biophys. Acta 1530 (1) (2001) 97–110.

[11] L.A. Kelley, M.J. Sternberg, Protein structure prediction on the Web: a case study using the Phyre server, Nat. Protoc. 4 (3) (2009) 363–371.

[12] E.E. Kooijman, K.N. Burger, Biophysics and function of phosphatidic acid: a molecular perspective, Biochim. Biophys. Acta 1791 (9) (2009) 881–888.

[13] R. Lavieri, S.A. Scott, et al., Design, synthesis, and biological evaluation of halogenated N-(2-(4-oxo-1-phenyl-1,3,8-triazaspiro[4.5]decan-8-yl)ethyl)benzamides: discovery of an isoform-selective small molecule phospholipase D2 inhibitor, J. Med. Chem. 53 (18) (2010) 6706–6719.

[14] N. Lehman, B. Ledford, et al., Phospholipase D2-derived phosphatidic acid binds to and activates ribosomal p70 S6 kinase independently of mTOR, FASEB J. 21 (4) (2007) 1075–1087.

[15] M. Liscovitch, M. Czarny, et al., Phospholipase D: molecular and cell biology of a novel gene family, Biochem. J. 345 (Pt 3) (2000) 401–415.

[16] M. Mahankali, G. Alter, et al., Mechanism of Enzymatic Reaction and Protein-Protein Interactions of PLD from a 3D Structural Model, Cell. Signal. 27 (2014) 69–81.

[17] L. Monovich, B. Mugrage, et al., Optimization of halopemide for phospholipase D2 inhibition, Bioorg. Med. Chem. Lett. 17 (8) (2007) 2310–2311.

[18] H. Oshimoto, S. Okamura, et al., Increased activity and expression of phospholipase D2 in human colorectal cancer, Oncol. Res. 14 (1) (2003) 31–37.

[19] H.J. Peng, K.M. Henkels, et al., Evidence for two CRIB domains in phospholipase D2 (PLD2) that the enzyme uses to specifically bind to the small GTPase Rac2, J. Biol. Chem. 286 (18) (2011) 16308–16320.

[20] C.P. Ponting, Novel domains in NADPH oxidase subunits, sorting nexins, and PtdIns 3-kinases: binding partners of SH3 domains? Protein Sci. 5 (11) (1996) 2353–2357.

[21] N. Saito, M. Ohata, et al., A case of unresectable colon cancer responding to oral leucovorin + oral tegafur/uracil, Gan To Kagaku Ryoho 34 (8) (2007) 1287–1290.

[22] V.A. Sciorra, S.A. Rudge, et al., Identification of a phosphoinositide binding motif that mediates activation of mammalian and yeast phospholipase D isoenzymes, EMBO J. 18 (21) (1999) 5911–5921.

[23] V.A. Sciorra, S.A. Rudge, et al., Dual role for phosphoinositides in regulation of yeast and mammalian phospholipase D enzymes, J. Cell Biol. 159 (6) (2002) 1039–1049.

[24] S.A. Scott, P.E. Selvy, et al., Design of isoform-selective phospholipase D inhibitors that modulate cancer cell invasiveness, Nat. Chem. Biol. 5 (2) (2009) 108–117.

[25] W. Su, Q. Chen, et al., Targeting phospholipase D with small-molecule inhibitors as a potential therapeutic approach for cancer metastasis, Future Oncol. 5 (9) (2009) 1477–1486.

[26] W. Su, O. Yeku, et al., 5-Fluoro-2-indolyl des-chlorohalopemide (FIPI), a phospholipase D pharmacological inhibitor that alters cell spreading and inhibits chemotaxis, Mol. Pharmacol. 75 (3) (2009) 437–446.

[27] O. Trott, A.J. Olson, AutoDock Vina: improving the speed and accuracy of docking with a new scoring function, efficient optimization, and multithreading, J. Comput. Chem. 31 (2) (2010) 455–461.

[28] D.S. Wang, G. Shaw, The association of the C-terminal region of beta I sigma II spectrin to brain membranes is mediated by a PH domain, does not require membrane proteins, and coincides with a inositol-1,4,5 triphosphate binding site, Biochem. Biophys. Res. Commun. 217 (2) (1995) 608–615.

[29] D.S. Wang, R. Shaw, et al., Binding of PH domains of beta-adrenergic receptor kinase and beta-spectrin to WD40/beta-transducin repeat containing regions of the beta-subunit of trimeric G-proteins, Biochem. Biophys. Res. Commun. 203 (1) (1994) 29–35.

[30] M.J. Wishart, G.S. Taylor, et al., Phoxy lipids: revealing PX domains as phosphoinositide binding modules, Cell 105 (7) (2001) 817–820.

[31] Y. Yamada, N. Hamajima, et al., Association of a polymorphism of the phospholipase D2 gene with the prevalence of colorectal cancer, J. Mol. Med. (Berl) 81 (2) (2003) 126–131.

[32] M. Yamazaki, Y. Zhang, et al., Interaction of the small G protein RhoA with the C terminus of human phospholipase D1, J. Biol. Chem. 274 (10) (1999) 6035–6038.

[33] L. Yao, Y. Kawakami, et al., The pleckstrin homology domain of Bruton tyrosine kinase interacts with protein kinase C, Proc. Natl. Acad. Sci. U. S. A. 91 (19) (1994) 9175–9179.

[34] Q. Ye, S. Kantonen, et al., A new signaling pathway (JAK-Fes-phospholipase D) that is enhanced in highly proliferative breast cancer cells, J. Biol. Chem. 288 (14) (2013) 9881–9891.

[35] Y. Zhang, I-TASSER server for protein 3D structure prediction, BMC Bioinforma. 9 (2008) 40.
[36] C. Zhao, G. Du, et al., Phospholipase D2-generated phosphatidic acid couples EGFR stimulation to Ras activation by Sos, Nat. Cell Biol. 9 (6) (2007) 706–712.
[37] J.A. Lewis, S.A. Scott, R. Lavieri, J.R. Buck, P.E. Selvy, S.L. Stoops, M.D. Armstrong, H.A. Brown, C.W. Lindsley, Design and synthesis of isoform-selective phospholipase D (PLD) inhibitors. Part I: impact of alternative halogenated privileged structures for PLD1 specificity, Bioorg. Med. Chem. Lett. 19 (2009) 1916–1920.